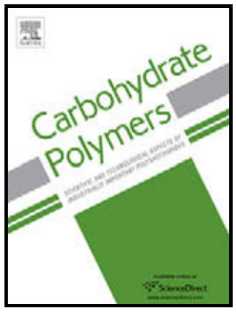

Title: Desiccation tolerance in plants: Structural characterization of the cell wall hemicellulosic polysaccharides in three *Selaginella* species

Authors: Barbara Plancot, Bruno Gügi, Jean-Claude Mollet, Corinne Loutelier-Bourhis, Sharathchandra Ramasandra Govind, Patrice Lerouge, Marie-Laure Follet-Gueye, Maïté Vicré, Carlos Alfonso, Eric Nguema-Ona, Muriel Bardor, Azeddine Driouich

PII: S0144-8617(18)31497-8
DOI: https://doi.org/10.1016/j.carbpol.2018.12.051
Reference: CARP 14405

To appear in:

Received date: 30 August 2018
Revised date: 16 November 2018
Accepted date: 17 December 2018

Please cite this article as: Plancot B, Gügi B, Mollet J-Claude, Loutelier-Bourhis C, Ramasandra Govind S, Lerouge P, Follet-Gueye M-Laure, Vicré M, Alfonso C, Nguema-Ona E, Bardor M, Driouich A, Desiccation tolerance in plants: Structural characterization of the cell wall hemicellulosic polysaccharides in three *Selaginella* species, *Carbohydrate Polymers* (2018), https://doi.org/10.1016/j.carbpol.2018.12.051

Original research paper

Desiccation tolerance in plants: structural characterization of the cell wall hemicellulosic polysaccharides in three *Selaginella* species.

Running title: ***Selaginella* cell wall analyses**

Barbara Plancot[1,2*], Bruno Gügi[1,2], Jean-Claude Mollet[1,2], Corinne Loutelier-Bourhis[3], Sharathchandra Ramasandra Govind [4], Patrice Lerouge[1,2], Marie-Laure Follet-Gueye[1,2], Maïté Vicré[1,2], Carlos Alfonso[3], Eric Nguema-Ona[1,2#], Muriel Bardor[1,2,5§] and Azeddine Driouich[1,2§]

From the [1]Normandie Univ, UniRouen, Laboratoire de Glycobiologie et Matrice Extracellulaire Végétale (Glyco-MEV), 76000 Rouen, France ; [2]Fédération de Recherche "Normandie-Végétal"-FED 4277, 76000 Rouen, France ; [3]Normandie Univ, UniRouen, CNRS UMR 6014, COBRA, 76000 Rouen, France; [4]Department of Studies and Research in Environmental Science. Tumkur University, Tumkur, Karnataka, 572103, India; [5]Institut Universitaire de France, Paris, France.

[#]present address: Centre Mondial de l'Innovation, Groupe Roullier, 35400, Saint-Malo, France.

*To whom correspondence should be addressed: Barbara Plancot: Normandie Univ, UniRouen, Laboratoire de Glycobiologie et Matrice Extracellulaire Végétale, 76000 Rouen, France; Fédération de Recherche "Normandie-Végétal"-FED 4277, 76000 Rouen, France; barbara.plancot@univ-rouen.fr.

(§) This work was co-supervised by MB and AD.

Corresponding author: Dr. Barbara Plancot (*)

Normandie Univ, UniRouen, Fédération de Recherche "Normandie-Végétal"-FED 4277, Laboratoire de Glycobiologie et Matrice Extracellulaire Végétale, bâtiment CURIB, 76821 Mont Saint Aignan. France

E-mail address: barbara.plancot@univ-rouen.fr

Highlights:

- Comparative structural characterization of leaf cell walls of desiccation-tolerant and desiccation-sensitive *Selaginella* species (*S. involvens vs S. kraussiana* and *S. moellendorffii)*.
- Leaf cell walls *Selaginella* species are mainly composed of hemicellulosic polysaccharides namely arabinoxylan, mannan and xyloglucan.
- Desiccation induces significant structural alterations of the xyloglucan and arabinoxylan in *S. involvens* compared to *S. kraussiana* and *S. moellendorffii*.

- Structural remodeling of these hemicellulosic polysaccharides is an important process leading to desiccation tolerance in *Selaginella* plants.

Abstract:

Drought-induced dehydration of vegetative tissues in lycopods affects growth and survival. Different species of *Selaginella* have evolved a series of specialized mechanisms to tolerate desiccation in vegetative tissues in response to water stress. In the present study, we report on the structural characterization of the leaf cell wall of the desiccation-tolerant species *S. involvens* and two desiccation-sensitive species, namely *S. kraussiana* and *S. moellendorffii*. Isolated cell walls from hydrated and desiccated leaves of each species were fractionated and the resulting oligosaccharide fragments were analyzed to determine their structural features. Our results demonstrate that desiccation induces substantial modifications in the cell wall composition and structure. Altogether, these data highlight the fact that structural remodeling of cell wall hemicellulosic polysaccharides including XXXG-rich xyloglucan, arabinoxylan and acetylated galactomannan is an important process in order to mitigate desiccation stress in *Selaginella*.

Key-words: cell wall, desiccation, hemicellulose, mannan, polysaccharide, xylan, xyloglucan.

1. Introduction

Water stress in the form of drought, dehydration and desiccation is a major limiting factor in global agricultural food production (Dinakar & Bartels, 2013). However, certain plants called "Resurrection plants" have developed adaptive strategies to withstand prolonged periods of dehydration and recover within a few hours to several days once water is available (Gaff & Ellis, 1974; Farrant & Moore, 2011; Gaff & Oliver, 2013; Charuvi et al., 2015). During dehydration and desiccation, cell wall folding plays an important role in cellular and mechanical stabilizations (Farrant, Brandt, & Lindsey, 2007). Furthermore, cell wall remodelling occurs in order to reduce mechanical strength thereby allowing the cell wall to fold and progressively adapt the cell shape (Moore, Vicré-Gibouin, Farrant, & Driouich, 2008). As water is lost from the cell, plasmolysis occurs resulting in plasma membrane tearing from the more rigid cell wall and ultimately leading to cell death. Resurrection plants have developed strategies to minimize the impact of mechanical stress to tolerate desiccation and subsequent cell death (Farrant, Vander Willigen, Loffell, Bartsch, & Whittaker, 2003). Desiccation tolerance is the ability to survive a severe water loss (>95%) for a long period of time (Moore, Le Brandt, Driouich, & Farrant, 2009). Interestingly, early studies on orthodox seeds have already highlighted the fact that the cell wall structural features are essential in conferring desiccation tolerance (Webb & Arnott, 1982). In fact, desiccation tolerant seeds exhibited highly undulated cell walls and a species-specific folding. The same authors also showed that the cell wall folding resulted from modifications of the cell wall composition and structure during desiccation (Webb & Arnott, 1982).

Lycophytes denote a key vascular plant lineage that includes Lycopodiaceae (club mosses), Isoetaceae (quillworts), and Selaginellaceae (spike mosses) (Yobi et al., 2012). *Selaginella* species represent an evolutionarily robust group of plants that were among the few to survive and thrive during the Permian-Triassic extinction (Banks, 2009). The oldest *Selaginella* fossil dates back to 400 million years ago (Banks et al., 2011). Species of *Selaginella* from the Upper Carboniferous are morphologically similar species of extant *Selaginella* (Banks, 2009). At the present time, only one genus is recognized in the Selaginellaceae. This genus contains approximately 700 species that occupy diverse habitats (temperate, tropical, frost-tolerant arctic, and drought-tolerant desert species) (Yobi et al., 2012; Banks, 2009). Several members of the *Selaginella* genus, including *S. lepidophylla* (Iturriaga, Cushman, & Cushman, 2006), *S. bryopteris* (Deeba, Pandey, Pathre, & Kanojiya, 2009) and *S. tamariscina* (Wang et al., 2010) have developed unique capabilities to withstand cellular

desiccation or by surviving complete air drying (Oliver, Tuba, & Mishler, 2000). On the other hand, poikilochlorophyllous plants lose totally or partially, their photosynthetic apparatus during the dehydration process (Yobi et al., 2013) and homoiochlorophyllous plants retain their chlorophyll and photosynthetic structures during desiccation. Like the latter plants, *Selaginella* species also retain their chlorophyll and presumably their photosynthetic capacities during desiccation (Moore et al., 2009). Similarly, *S. lepidophylla* maintains all its cellular organelles and membrane integrity during the dry state (Thomson & Platt, 1997). The role of the cell wall in desiccation tolerance in vascular plant lineage that diverged over 400 million years ago is relevant as these primitive plants have developed adaptive mechanisms that mitigate desiccation tolerance. Therefore, understanding these responses and tolerance mechanisms might provide novel strategies for the improvement of drought tolerance in crops with a potential to improve productivity in an ever-changing micro-climactic conditions (Pampurova & Van Dijck, 2014).

Xyloglucan (XyG) is a major hemicellulosic polysaccharide of the primary cell wall of eudicots where it binds cellulose microfibrils to forms a network which controls cell growth (Han, Li, Li, Zhao, & Wang, 2012; Cosgrove, 2005). Classical XyG structure consists of a β-(1,4)-D-glucan backbone substituted with xylose (D–Xyl), galactose-xylose (D-Gal-D-Xyl) or fucose-galactose-xylose (L-Fuc-D-Gal-D-Xyl) motifs. A nomenclature using one-letter code for the different sidechain oligosaccharides has been proposed by Fry et al., (1993) in which G represents the unsubstituted β-glucosyl residue, whereas X, L and F represent α-D-Xyl*p*-(1,6)-β-D-Glc*p*, β-D-Gal*p*-(1,2)-α-D-Xyl*p*-(1,6)-β-D-Glc*p* and α-L-Fuc*p*-(1,2)-β-D-Gal*p*-(1,2)-α-D-Xyl*p*-(1,6)-β-D-Glcp respectively (Fry et al., 1993). Furthermore, these structures can be *O*-acetylated. Reports suggest that *O*-acetylation has affects polymer properties. Moreover, the degree of *O*-acetylation was correlated with an increase of polymer resistance to enzymatic hydrolysis by glycosyl hydrolases (Pauly & Ramírez, 2018). XyG fine structure displays variations within vascular plants which might be used as markers for taxonomic lineage (Hsieh & Harris, 2012). In the lycophyte *S. kraussiana*, the XyG profiles present abundant oligosaccharides containing arabinosyl residues such as α-L-Ara*f*-(1,2)-α-D-Xyl*p*-(1,6)-β-D-Glc*p*, α-L-Ara*p*-(1,2)-α-D-Xyl*p*-(1,6)-β-D-Glc*p* and α-L-Fuc-(1,2)-α-L-Ara*p*-(1,2)-α-D-Xyl*p*-(1,6)-β-D-Glc*p* that correspond to S, D and E respectively (Pena, Darvill, Eberhard, York, & O'Neill, 2008; Schultink et al., 2014). In fact, XyG-specific *endo* β-(1,4)-glucanase treatment on XyG released small proportions of fucogalactoXyG and large proportions of arabinoXyG from *S. kraussiana* (Pena et al., 2008; Pauly & Keegstra, 2016). In contrast, XyG profiles from other *Selaginella* species are currently unknown. In *Craterostigma wilmsii*, the structure and distribution of XyG in leaf cell walls was affected by desiccation (Vicré, Sherwin, Driouich,

Jaffer, & Farrant, 1999; Vicré, Farrant, & Driouich, 2004). The authors have found a significant increase in XyG epitopes in the cell wall using immunomicroscopy. In the related species *C. plantagineum*, an up-regulation of gene expression corresponding to *EXPANSIN*, XyG endotransglucosylase/hydrolase (*XTH*) and xyloglucosyl transferase was reported during desiccation (Jones & McQueen-Mason, 2004; Rodriguez et al., 2010). These data suggest that the cleavage by XyG-modifying enzymes releases the tightly bound XyG-cellulose network thus increasing cell wall flexibility required for the cell wall folding upon desiccation. In contrast, XyG profiles of other *Selaginella* species are currently unknown.

In monocot, XyG can be found in low amount as compared to xylan (Hsieh & Harris, 2012). For example, it has been shown that Ara and Xyl were the major monosaccharides in cell walls of *Eragrostis nindensis*, a monocot resurrection plant, suggesting the presence of high levels of arabinoxylan (AX) (Moore et al., 2013). The backbone of such polymers consists of β-(1,4)-D-xylopyranosyl residues that can be *O*-acetylated and branched with one or two L-arabinosyl residues (Scheller & Ulvskov, 2010). In addition, the xylan/AX structure can also be substituted with D-glucuronic acid (GlcA) and/or its 4-*O*-methyl derivative (Glucuronoarabinoxylan: GAX) and linked to ferulic acid (Fry & Ulvskov, 2011). Mannan polysaccharides are widespread among land plants and are also present in many algal species, some of which completely lacking cellulose in their cell walls (Frei & Preston, 1968). Several mannan polysaccharides have been characterized, including pure mannan, galactomannan, glucomannan, and galactoglucomannan (Liepman et al., 2007). Structurally, each of these polysaccharides contains linear or branched polymers containing monosaccharides such as D-mannose (Man), D-Gal, and D-Glucose (Glc) and may be substituted with α-(1,6)-linked Gal side chains and are partially substituted by *O*-acetyl groups.

So far, very little information is available on the cell wall composition and structure of the *Selaginella* species during desiccation. The present study reports on the structural characterization of hemicellulosic polysaccharides namely XyG, xylans, and mannans in, desiccation-tolerant *S. involvens*, and two desiccation-sensitive *Selaginella* species: *S. kraussiana* and *S. moellendorffii*, respectively. The analyses were performed on hydrated and desiccated leaves in order to determine the cell wall structural changes related to desiccation tolerance. We hypothesize that the structural remodeling of hemicellulosic polysaccharides is an important process that could control mechanical properties of the cell wall during desiccation of *Selaginella* species.

2. Materials and Methods

2.1. Materials

2.1.1. Plants and desiccation

S. moellendorffii was obtained from the nursery "FLOSAB.com Vivaces et plantes Alpines, http://www.flosab.com/" and *S. involvens* and *S. kraussiana* were purchased at the nursery "Le monde des fougères, http://pepiniereezavin.com/" and maintained under 50% humidity with natural sun light (<1000 mol m−2 s−1 photosynthetic photon flux density). Fronds from three different pots were detached and subjected to desiccation. The fronds were kept on Petri dishes and allowed to air dry at 25 °C and <20 µmol m^{-2} s^{-1} photosynthetic photon flux density for about 12 h. This was adapted from (Pandey et al., (2010). All plants were still alive when prepared for the experiments as illustrated in Fig. 1.

2.1.2. Chemicals

α-amylase and amyloglucosidase (EC 3.2.1.1, Megazyme, USA), 2,5-dihydroxybenzoic acid (DHB, Sigma-Aldrich, UK), acetic acid glacial (Fisher-Scientific, UK), acetone (Fisher-Scientific, United State), acetonitrile (Sigma-Aldrich, UK), ammonium acetate (Sigma-Aldrich, Japan), adhesive Carbon Tabs 12 mm (Agar Scientific, UK), ammonium oxalate (Sigma-Aldrich, India), arabinan from sugar beet (Megazyme, Ireland), arabinoxylan from wheat (Megazyme, USA), chloroform (Alfa Aesar, Germany), cyclohexane (Acros Organic, Belgium), *endo*-(1,4)-β-D-glucanase (EC 3.2.1.4; Megazyme, Ireland), *endo*-(1,4)-β-D-xylanase (EC 3.2.1.8; Megazyme, Ireland) or *endo*-(1,4)-β-D-mannanase (EC 3.2.1.78; Megazyme, Ireland), ethanol (VWR, France), arabinogalactan of gum arabic from acacia (Fisher-Scientific, UK), galactomannan from *Ceratonia siliqua* seeds (Sigma-Aldrich, USA), hexamethyldisilizane: trimethylchlorosilane: pyridine (Supelco, USA), inositol (Sigma-Aldrich, China), *Iso*-propanol (Merck, Germany), KOH (Fisher-Scientific, UK), methanol (Fisher-Scientific, United State), methanol:HCl (Supelco, USA), $NaBH_4$ (Merck, Germany), NaCl (Alfa Aesar, Germany), nitrocellulose membrane 0.2 µm (GE Healthcare Life Science, Germany), goat anti–mouse IgG (whole molecule) antibody conjugated with alkaline phosphatase (Thermo Scientific, USA), goat anti–rat IgG (whole molecule) antibody conjugated with alkaline phosphatase (Thermo Scientific, USA), trifluoroacetic acid (TFA, Thermo Scientific, USA), Tris-HCl (Fisher Scientific, UK), tween 20 (Acros Organic, Belgium), larchwood xylan (Sigma-Aldrich, USA) and tamarind XyG (Megazyme, Ireland) were used.

LM (Leeds Monoclonal) mAbs were purchased from Plant Probes (Leeds, UK); CCRC-M1 (Complex Carbohydrate Research Center-Monoclonal1) was purchased from Agrisera (Sweden).

2.2. Methods

2.2.1. Scanning electron microscopy

Scanning electron microscopy was performed with a SEM Hitashi TM 3000 Tabletop microscope equipped with a Deβen cooling stage. Samples were observed at 15 kV and images were acquired in analytical mode. The samples were observed without coating and on Leit Adhesive Carbon Tabs 12mm. For hydrated samples, the cooling stage was set at -20 °C and desiccated plants were observed at room temperature. The images were acquired at 50x and 500x magnifications.

2.2.2. Preparation of the Alcohol Insoluble Residue (AIR)

Leaves from hydrated and desiccated plants were frozen in liquid N_2 and freeze-dried as previously described (Vicré, Lerouxel, Farrant, Lerouge, & Driouich, 2004; Moore et al., 2013). Freeze dried leaves were ground to a fine powder in a mortar and suspended three times in boiling ethanol 70% at 70 °C for 15 min. Series of extractions were performed to remove lipids, polyphenols, and low molecular weight metabolites from the cell wall containing residues. Briefly, the residues were extracted twice with methanol-chloroform (1:1; v/v), twice with methanol-acetone (1:1; v/v) and finally with methanol-water (1:1; v/v) for 2 h each at room temperature under agitation. The insoluble residue was resuspended in 50 mM ammonium acetate, pH 5.4, and starch was removed at 80 °C using a thermostable α-amylase and amyloglucosidase (10U) for 24 h. After dialysis against de-ionized water, cell wall residues were freeze-dried. This corresponds to total cell wall fraction also known as alcohol insoluble residue (AIR).

2.2.3. Fractionation of cell wall material

Fractions of AIR were subjected to sequential extractions as previously described by Moore et al., (2013). Pectins were extracted as follows: lyophilized AIR was treated with 0.5% of ammonium oxalate (w/v), for 1h at 100 °C. After centrifugation for 10 min at 10,000 *g*, the supernatant was dialyzed against de-ionized water. The insoluble fraction was then treated with 4 M KOH containing 20 mM $NaBH_4$ overnight at room temperature. The pH of the supernatants was adjusted to pH 5.5 with glacial acetic acid. Then, the supernatant was centrifuged for 10

min at 3,500 *g*, dialyzed against de-ionized water and freeze-dried giving the hemicellulose-enriched fraction. The pellet was washed several times with de-ionized water and freeze-dried yielding the "cellulosic residue". All lyophilized materials were stored at room temperature. The cell wall fractionation procedure was carried out in triplicate for each condition.

2.2.4. Composition analyses of cell wall fractions

Monosaccharide composition of each cell wall fraction was analyzed by gas chromatography coupled to a Flame Ionization Detector (GC-FID) spiking 50 µl of inositol 2 mM as an internal standard. Each fraction (1 mg) was subjected to hydrolysis with 2 M trifluoroacetic acid (TFA) for 2 h at 110 °C. TFA was washed twice with a 50% *iso*-propanolwater solution. The released monosaccharides were converted to their *O*-methyl glycosides by incubation in 1 M methanol:HCl at 80 °C overnight (Moore et al., 2006). The methyl glycosides were then converted into their trimethylsilyl derivatives by heating the samples for 20 min at 110 °C in hexamethyldisilazane:trimethylchlorosilane:pyridine (3/1/9). After evaporation of the reagent, the samples were suspended in cyclohexane before being injected on a CP-Sil 5 CB column (Agilent Technologies). Chromatographic data were integrated with GC Star Workstation software (Varian). A temperature program (3 min at 40 °C; up to 160 °C at 15 °C min^{-1}; up to 220 °C at 1.5 °C min^{-1}; up to 280 °C at 20 °C min^{-1}; 3 min at 280 °C) optimized for the separation of the most common cell wall authentic monosaccharides such as arabinose (Ara), rhamnose (Rha), fucose (Fuc), xylose (Xyl), glucuronic acid (GlcA), mannose (Man), galactose (Gal), galacturonic acid (GalA) and glucose (Glc).

2.2.5. Slot-blot immunoassays

Immunoslot-blot assays were performed after blotting 10 µg of extract under vacuum onto a nitrocellulose membrane (0.2 µm mesh). The membrane was blocked overnight at room temperature using Tris-buffered saline (Tris-HCl 10 mM; NaCl 0.5 M) containing 1% (v/v) Tween 20 (TBST). The primary monoclonal antibodies (mAb) were diluted 1:50 in TBST (Mollet, Park, Nothnagel, & Lord, 2000). Weakly substituted xylan and more extensively branched arabinoxylan were detected with the LM10 and LM11 mAbs, respectively (McCartney, Marcus, & Knox, 2005), fucosylated and galactosylated XyG were detected with CCRC-M1 and LM25 mAbs, respectively (Puhlmann et al., 1994; Pedersen et al. 2012). Heteromannan was detected with the LM21 mAb (Marcus et al., 2010). Arabinan from sugar beet, xylan from larchwood, arabinoxylan from wheat, XyG from tamarind, arabinogalactan of gum arabic from acacia and galactomannan from *Ceratonia siliqua* seeds were used as controls.

The membrane was washed three times in TBST for 10 min each. The binding of the mAb was revealed with a goat anti–rat IgG (whole molecule) antibody diluted 1:1,000 for LM10, LM11, LM21 and LM25; with a goat anti–mouse IgG (whole molecule) antibody diluted 1:1,000 for CCRC-M1 and *Western Blue® Stabilized Substrate for Alkaline Phosphatase* (Fisher Scientific*)*.

2.2.6. Analysis of XyG, Xylan and Mannan oligosaccharides by matrix-assisted light desorption ionization-time of flight mass spectrometry (MALDI-TOF MS)

Five mg of cell wall samples (AIR or hemicellulose-enriched) were incubated under agitation for 16 h at 37 °C with either an *endo*-(1,4)-*β*-D-glucanase (5 U), *endo*-(1,4)-*β*-D-xylanase (10 U) or *endo*-(1,4)-β-D-mannanase (5 U) prepared in 10 mM ammonium acetate buffer, pH 5. After digestion, 4 V of ethanol were added and samples were kept, stored at -20 °C overnight and then centrifuged at 10,000 *g* for 10 min. The supernatants containing the oligosaccharides were concentrated by evaporation under a stream of air. The oligosaccharides were analyzed by MALDI-TOF-MS. Spectra were acquired on a Voyager DE-Pro instrument (Applied Biosystems) equipped with a 337-nm nitrogen laser. MS was performed in the reflector delayed extraction mode using 2,5-dihydroxybenzoic acid (DHB) as a matrix. Dried-droplet samples were prepared by spotting 1 µL of a mixture of DHB as a matrix (10 mg mL^{-1} in 0.1% TFA: acetonitrile (7:3)) and 1 µL of the sample on the target plate. The spectra were recorded in positive mode using an acceleration voltage of 20,000 V with a delay time of 100 ns and above 50% of the laser energy. They were externally calibrated using commercially available mixtures of peptides and proteins. Laser shots were accumulated for each spectrum in order to obtain an acceptable signal-to-noise ratio (sum of 10 spectra of 1,000 shots per spectrum). Digestion of XyG from tamarind, xylan from larchwood, AX from wheat and galactomannan from *Ceratonia siliqua* seeds were used as controls.

2.2.7. Determination of relative abundance of XyG, Xylan and Mannan oligosaccharides after MALDI-TOF MS analysis

The relative abundance of each ion was determined by measuring each individual ion-signal of XyG, xylan and mannan oligosaccharides and divided them by the sum of all ion-signals. The results were then expressed as a relative percentage.

2.2.8. Analysis of XyG and Xylan oligosaccharides by ElectroSpray Ionisation/ MS^n ($ESI\text{-}MS^n$)

The XyG and AX were also analyzed by $ESI\text{-}MS^n$ (n=1 to 4) using a Bruker HCT Ultra ETD II quadrupole ion-trap (QIT) mass spectrometer equipped with Esquire control 6.2 and Data Analysis 4.0 software (Bruker Daltonics, Bremen, Germany) (Plancot et al., 2014). For the ESI parameters, the capillary and end plate voltages were respectively set at – 3.5 kV and – 3.0 kV in positive ion mode. The capillary exit voltage was adjusted between 140 V and 200 V (depending of the *m/z* value) and the skimmer voltage was set at 40 V. The nebulizer gas (N_2) pressure, drying gas (N_2) flow rate and drying gas temperature were 10 psi, 7.0 L min^{-1} and 300 °C, respectively. Helium pressure in the ion trap was 1.4×10^{-5} mbar. The *m/z* range was 200-2200, using a scan speed of 8,100 *m/z* per second. The number of ions entering the trap cell was automatically adjusted by controlling the accumulation time using the ion charge control (ICC) mode (target 100,000) with a maximum accumulation time of 50 ms. The injection low-mass cut-off (LMCO) value was either *m/z* 120 or *m/z* 140, depending on the *m/z* value. The values of spectra average and rolling average were 6 and 2 respectively. $ESI\text{-}MS^n$ experiments were carried out by collision-induced dissociation (CID) using helium as the collision gas, isolation width of 1.5 *m/z* unit for the precursor ions and of 2 *m/z* unit for the intermediate ions and using a resonant excitation frequency with an amplitude from 0.8 to 1.0 $V_{p-p.}$ Sample solutions were infused into the source at a flow-rate of 3 µL min^{-1} by means of a syringe pump (Cole-Palmer, Vernon Hills, Illinois, USA).

2.2.9. Statistical analyses

Two comparisons were used to confirm statistical significance. Data were first compared by a *t*-test to compare two by two hydrated and desiccated *S. moellendorffii*, hydrated and desiccated *S. involvens* and hydrated and desiccated *S. kraussiana*. Then, data were compared by ANOVA multiple comparisons (Kruskal-Wallis test, GraphPad Software, Inc, La Jolla, CA, USA) ($P < 0.05$). For Gas-chromatography experiments, 3 independent extractions with at least three technical replicates per experiment were carried out. For the mass-spectrometry experiments, 3 independent extractions per experiment were carried out.

3. Results and discussion

3.1. *Selaginella* leaves undergo morphological alterations upon desiccation

Three *Selaginella* species, *S. moellendorffii*, *S. involvens*, and *S. kraussiana*, were collected under hydrated and desiccated conditions and photographed (Fig. 1). The leaves of desiccated plants (all three species) exhibited various degrees of curling without completely losing their green color (*i.e.* retention of their chlorophyll) (Fig. 1). Further analysis of the plants using scanning electron microscopy (SEM) confirmed the leaf folding (Fig. 2).

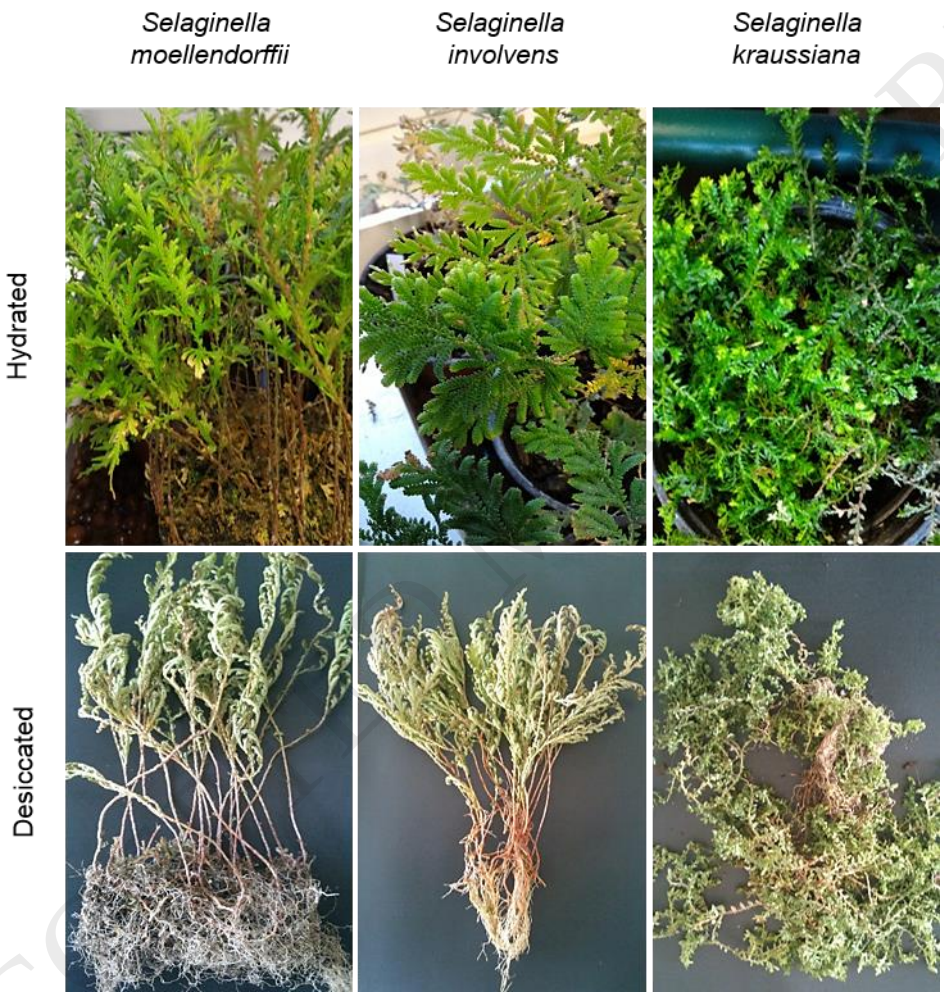

Fig 1. Photographs of the three *Selaginella* species used in the present study (hydrated and desiccated plants are shown).

In addition, microscopic observations of the epidermal surface of hydrated leaves in *S. involvens*, *S. kraussiana* and *S. moellendorffii* revealed the presence of numerous stomata between regular epidermal cells (Fig. 2B, 2F, 2J, 2L). Comparative SEM analysis of epidermal cells in hydrated and desiccated leaves of the three species revealed significant folding of the

cell walls upon desiccation (Fig. 2A-L). Cell wall folding was much more pronounced in *S. kraussiana* and *S. involvens,* than in *S. moellendorffii* (Fig. 2D, 2H, 2L). The same phenomenon has been observed in many other resurrection angiosperm plants. (Moore et al., 2006; Moore et al., 2008; Moore et al., 2009; Moore et al., 2013; Vicré et al., 2004). *Selaginella* species also undergo folding of their leaf cell walls during desiccation. The observed folding is most likely related to structural changes of the cell wall in response to desiccation. Furthermore, the cell wall folding has always been correlated with changes in polysaccharide and proteoglycan structures in several angiosperm resurrection plants (Moore et al., 2006; Vicré et al., 2004). For this reason, we decided to focus on the study of the cell wall of *Selaginella,* key vascular plants lineage, during desiccation.

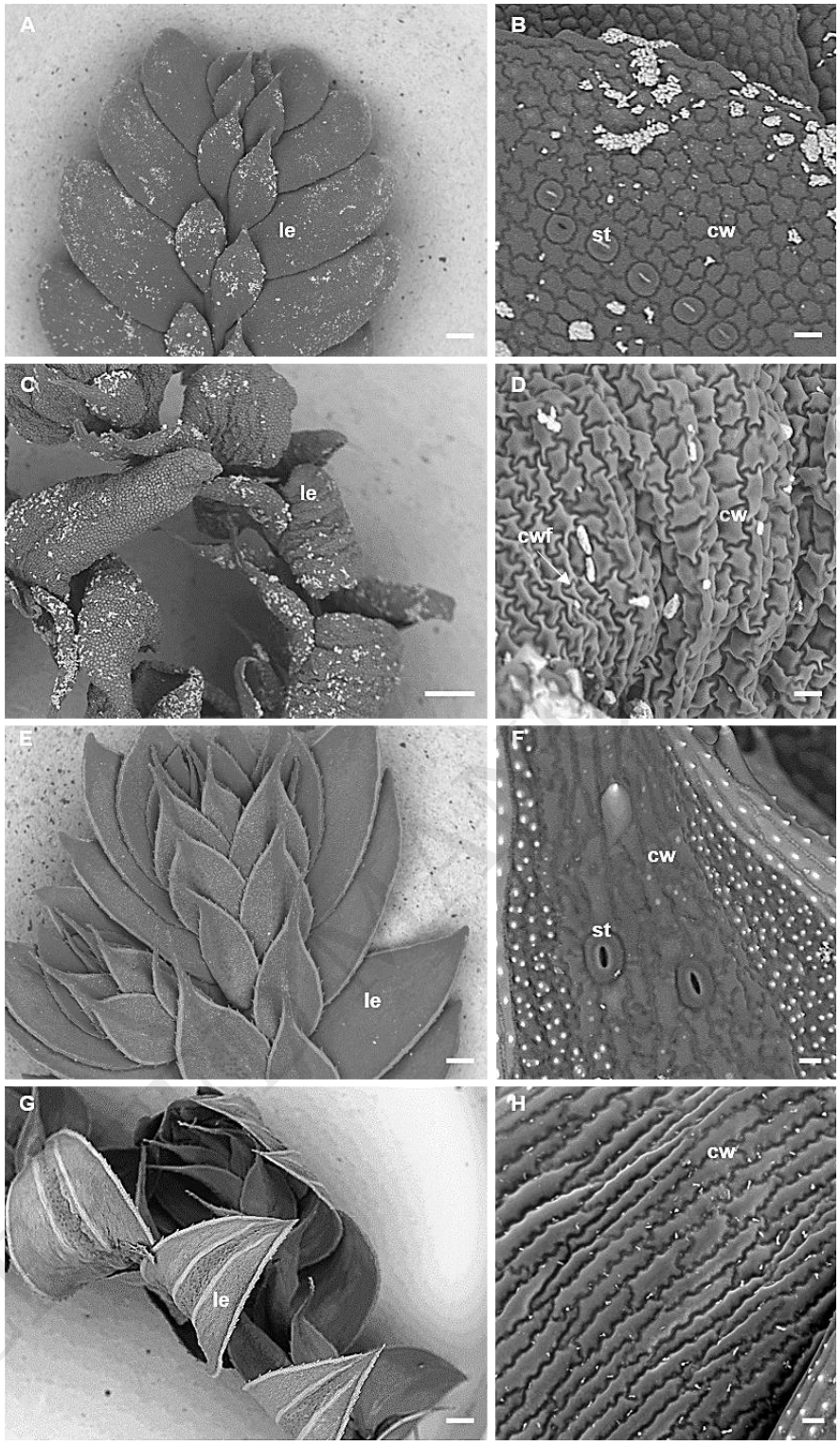

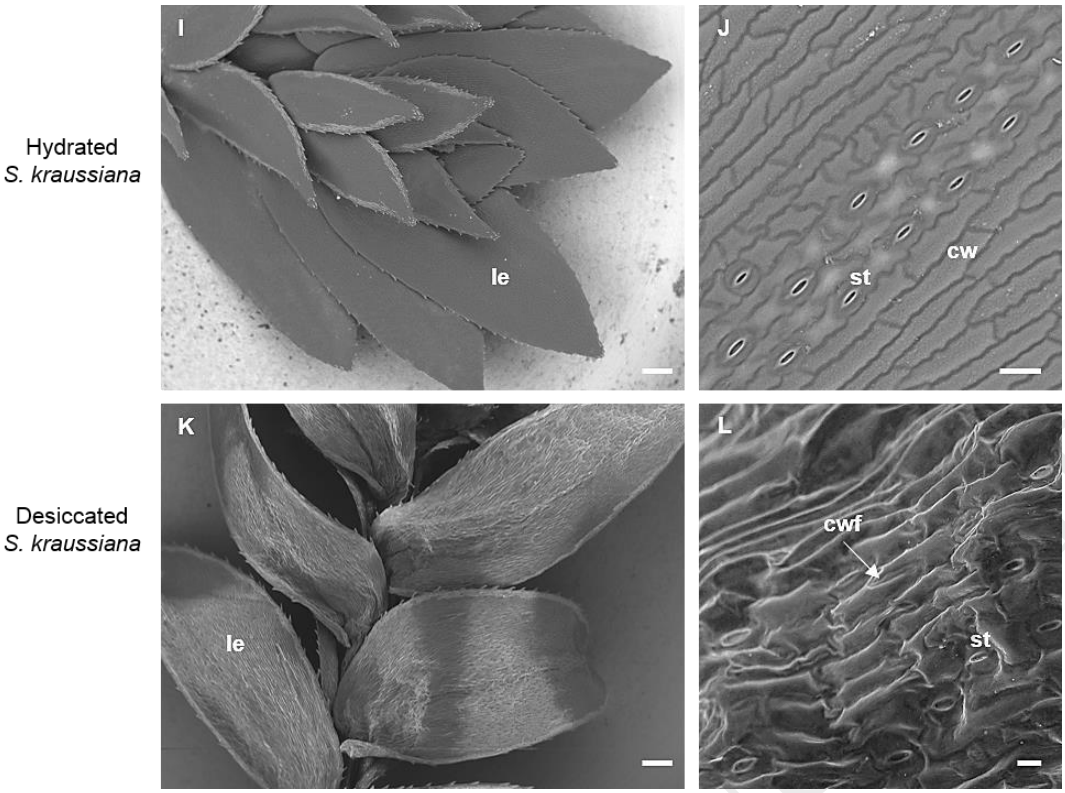

Fig 2. Scanning electron micrographs of upper surface of hydrated (A, B, E, F, I, J) and desiccated (C, D, G, H, K, L) of leaves from *S. involvens, S. moellendorffii* and *S. kraussiana*. General view of the epidermal surface of hydrated and desiccated leaves (A, C, E, G, I, K) and close up(B, D, F, H, J, L). cw, cell wall; cwf →, cell wall folding; le, leaf; st, stomata. Scale bars: A, C, E, G, I and K = 200 μm; B = 20 μm; D, F, H and L = 10 μm; J = 30 μm.

3.2. Monosaccharide composition of leaf cell walls of three *Selaginella* species under hydrated and desiccated conditions

To investigate the relationship between cell wall folding and structure, we first analyzed the monosaccharide composition of the cell wall of both hydrated and desiccated leaves of the three *Selaginella* species. Monosaccharide composition of the leaf-derived AIR (Alcohol Insoluble Residues) from the three species studied, showed that the trifluoroacetic acid (TFA)-soluble fractions predominantly consisted of Xyl, Ara and Man (nearly 70% of total monosaccharide content; Fig. 3). It is known that these three residues are present in hemicellulosic polysaccharides from arabinoxylan, mannan, and XyG. It is worth noting that the desiccation-tolerant plant *S. involvens* displayed the highest levels of both Xyl and Ara and the lowest level of Man as compared to the two other species. The level of Xyl was similar in both hydrated and desiccated leaves of *S. involvens* and the desiccation-sensitive *S. moellendorffii* species. In contrast, the level of Xyl in *S. kraussiana* increased significantly in desiccated leaves. The level of Ara increased significantly in desiccated leaves of *S. involvens*

but did not change after desiccation in *S. moellendorffii* and *S. kraussiana*. Similarly, the level of Man did not change under desiccated condition in these two species, while it increased in *S. involvens*. These modifications foreshadow modifications of the hemicellulosic polysaccharides in the cell wall. Therefore, we fractionated the cell wall extracts of *Selaginella* species and focused on XyG, xylan and mannan or combinations thereof.

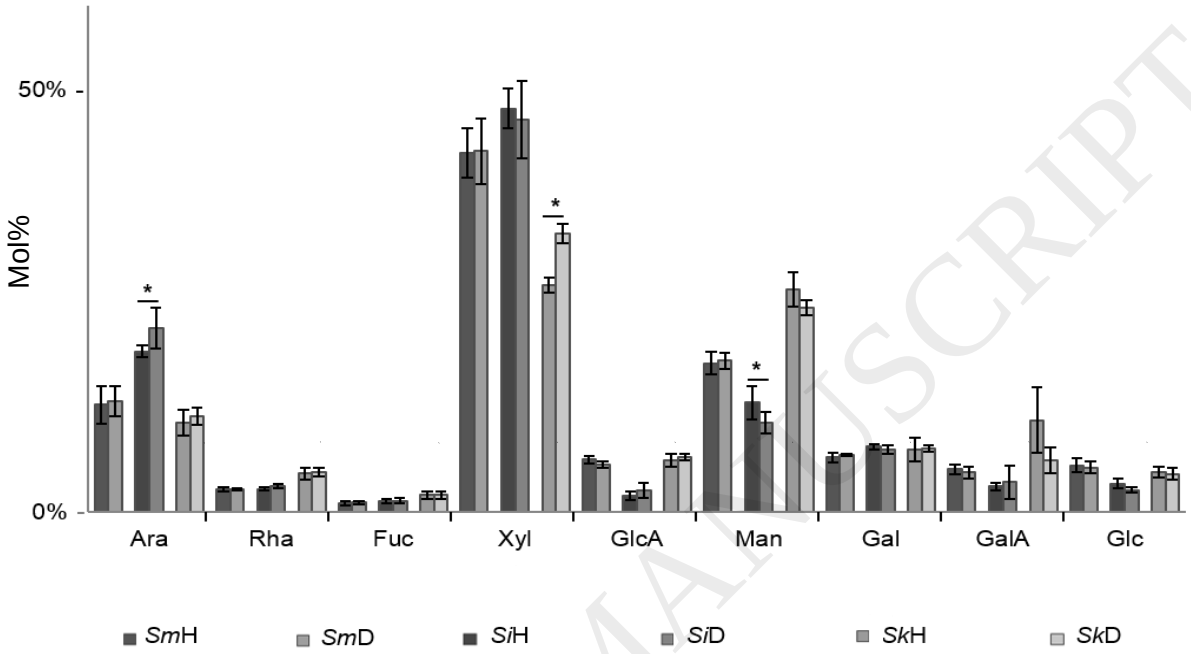

Fig 3. Monosaccharide composition of the AIR from hydrated and desiccated leaves in the the three *Selaginella* species.
Ara, arabinose; Rha, rhamnose; Fuc, fucose; Xyl, xylose; GlcA, glucuronic acid; Man, mannose; Gal, galactose; GalA, galacturonic acid; Glc, glucose. Bars represent the mean ± SE from 3 independent extractions with at least three technical replicates per experiment. Star indicates significant difference at $p < 0.05$ (Mann-Whitney test).
*Sm*H, hydrated *S. moellendorffii; Sm*D, desiccated *S. moellendorffii*; *Si*H, hydrated *S. involvens*; *Si*D, desiccated *S. involvens*; *Sk*H, hydrated *S. kraussiana; Sk*D, desiccated *S.*

3.3. Monosaccharide composition of the hemicellulose-enriched cell wall extracts

Monosaccharide composition of the hemicellulose-enriched fractions revealed that Xyl and Ara are the major sugars in the three species (Fig. 4). Xyl and Ara residues represented 55% to 64% respectively of the total monosaccharides. Xyl content did not differ significantly between desiccated and hydrated plants. In contrast, Ara content increased significantly in the desiccated leaves of *S. involvens* but not in the two other species.

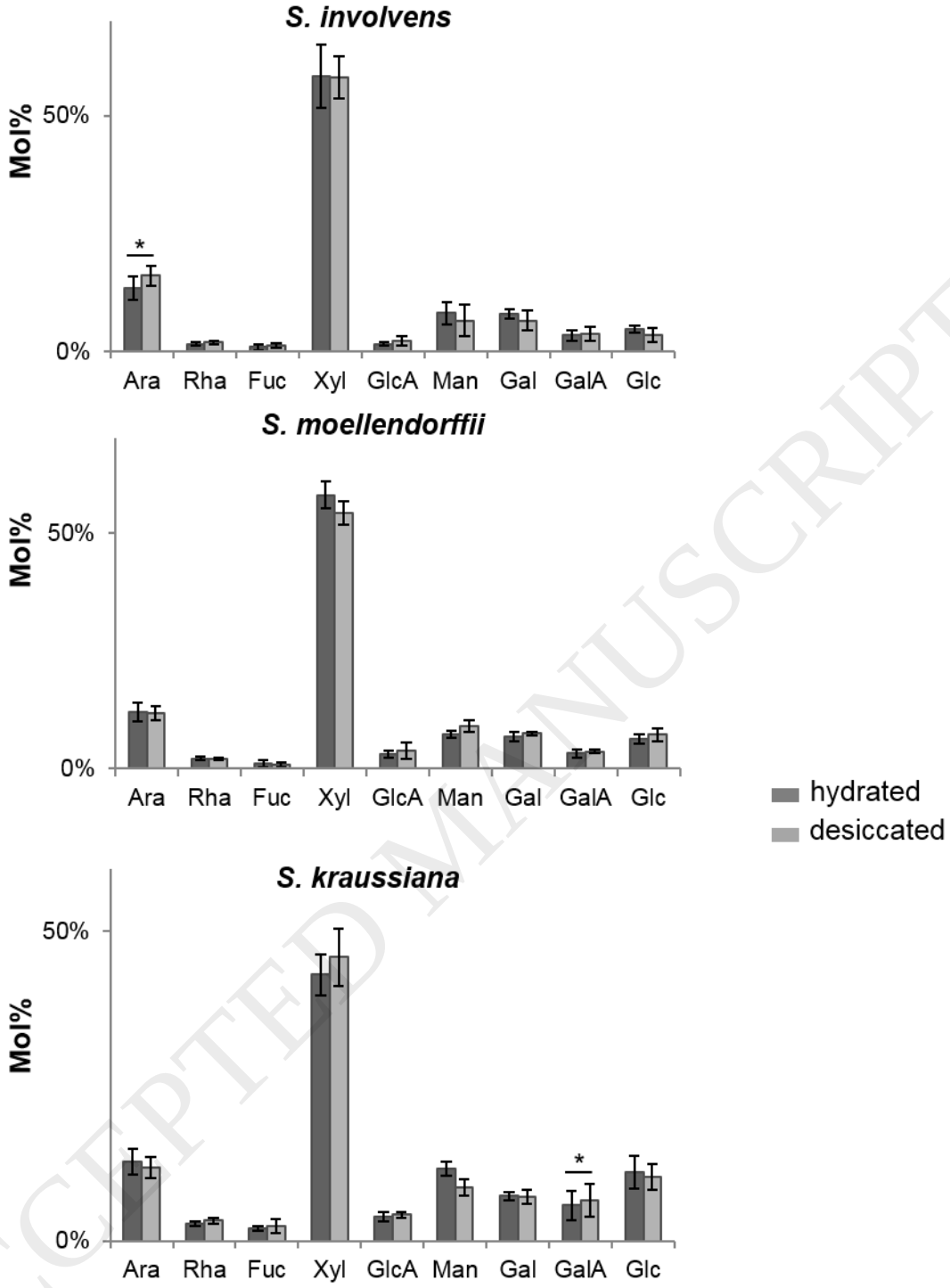

Fig 4. Monosaccharide composition of the hemicellulose-enriched cell wall fractions from *S. moellendorffii*, *S. involvens* and *S. kraussiana* hydrated and desiccated leaves. Ara, arabinose; Rha, rhamnose; Fuc, fucose; Xyl, xylose; GlcA, glucuronic acid; Man, mannose; Gal, galactose; GalA, galacturonic acid; Glc, glucose. Bars represent the mean ± SE (n=3 different cell wall extracts with at least three technical replicates per experiment). Stars indicate significant difference at $p < 0.05$ (Mann-Whitney test).

The presence of Xyl, Ara, Glc and Gal is indicative of the occurrence of AX and XyG which was further confirmed by immunoslot-blot assays using anti-XyG and anti-AX specific antibodies, namely LM25, CCRC-M1, LM10 and LM11 (Fig. S1, Fig. S2).

Our data suggest that xylan, AX and possibly XyG are major components of the hemicellulose-enriched KOH fraction. Mannan (and/or Galactomannan) were also present. Next, we further characterized the structure of these polymers using OLIMP (OLIgosaccharide Mass Profiling) by enzymatic digestion and MALDI-TOF mass spectrometry as previously described (Lerouxel et al., 2002; Ray et al., 2004; Moore et al., 2006; Mouille et al., 2006 ; Gribaa et al., 2013).

3.4. Structural analyses of Xylan

To gain information on the level of branching of the arabinoxylan polymers, the Ara/Xyl ratio in hemicellulosic-enriched fraction was compared in the three species (Fig. S3). Our data show consistently that the Ara levels are higher in the desiccated *S. involvens* plants as compared to the hydrated ones. The substitution level of the xylan backbone by arabinosyl residues (molar Ara/Xyl ratio) is low and similar in hydrated and desiccated *S. moellendorffii* (0.22 and 0.25). Comparatively, the level of substitution is higher in *S. kraussiana* (0.30) but decreases after desiccation (0.25). In contrast, the Ara/Xyl ratio in the desiccation-tolerant species *S. involvens* (0.19) is very low as compared to the two other species but increases significantly after desiccation (0.28). In desiccated conditions, the Ara/Xyl ratio increased in *S. involvens* while it decreased in *S. kraussiana* indicating a significant modification of the xylan structure, especially in terms of branching. In addition, xylan from *S. kraussiana* is highly substituted relative to that of the two other species. Moore and co-workers (2012) have shown that xylan was also an abundant cell wall component in resurrection plant grasses. These polymers were more arabinosylated in dehydrated than in hydrated plants. These data suggest that structural changes may modulate the mechanical properties of the cell wall to avoid cell tearing during dehydration (Moore et al., 2006; Liepman et al., 2007). More specifically, in the cell wall, xylan can interact with cellulose microfibrils contributing to the cell wall mechanical properties and increasing wall rigidity. Xylan is known to regulate cellulose-xylan association (Busse-Wicher, Grantham, Lyczakowski, Nikolovski, & Dupree, 2016) and the high level of xylan substitution observed in our study also might impact this association in *Selaginella*. This would allow maintaining a higher extensibility of the cell wall during dehydration (Moore et al., 2013). Together, these data suggest that, among other cell wall components, xylan structure is modulating the impact of mechanical stress avoiding irreversible damages during desiccation (Vicré et al., 2004; Moore et al., 2012).

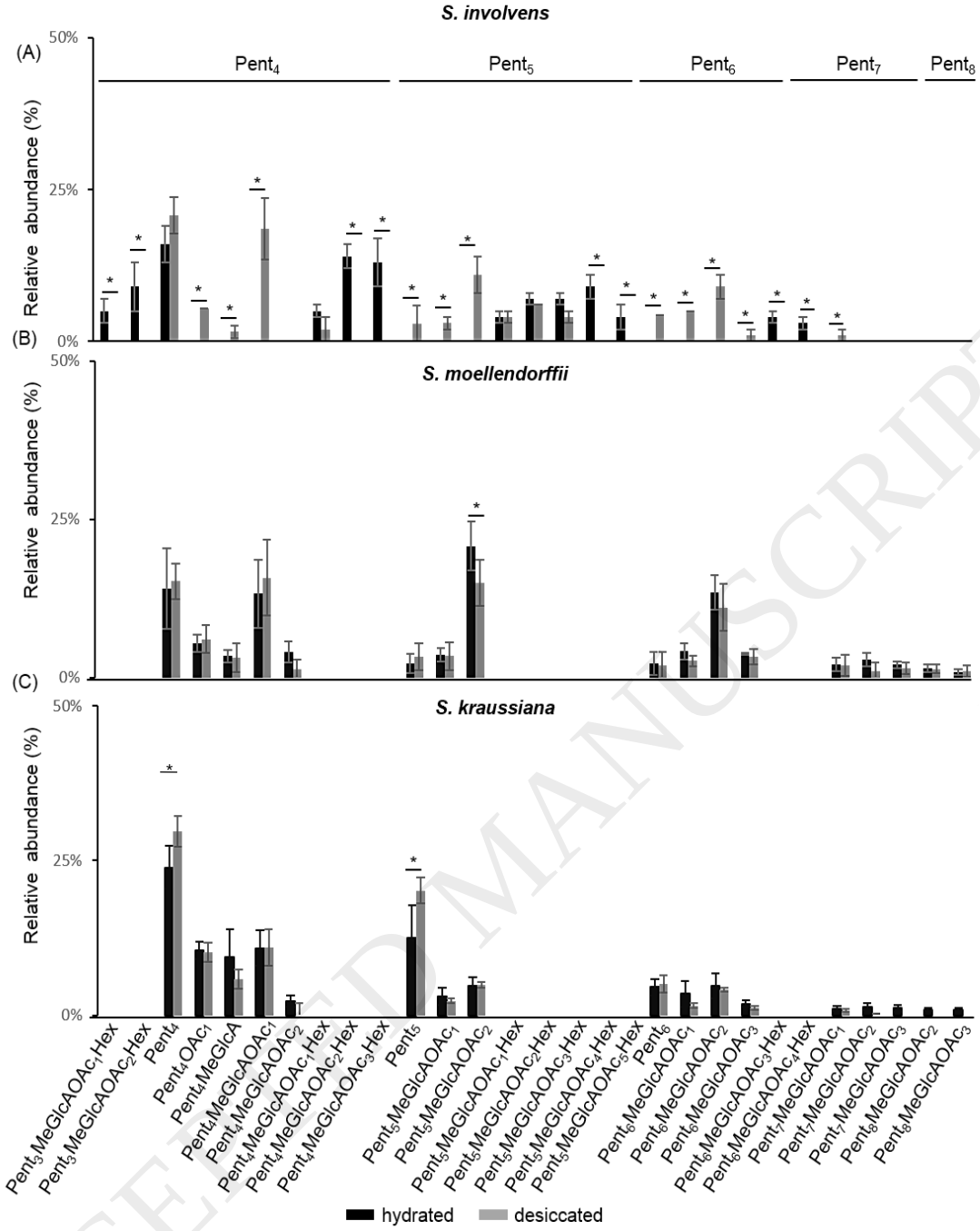

Fig 5. Relative quantification of xylan oligosaccharides obtained after *endo*- β-(1,4)-D-xylanase digestion of the total cell wall of *S. involvens* (A); *S. moellendorffii* (B) and *S. kraussiana* (C). Arabinoxylan oligosaccharides generated after the digestion were analyzed by MALDI-TOF / Mass Spectrometry. Data are presented as mean ±SE (n = 3 different cell wall extracts). Stars indicate significant difference at $p < 0.05$.
Hex, hexose; Pent, pentose; MeGlcA, 4-*O*-methylglucuronic acid; OAc, *O*-acetyl.

To investigate the structure of xylan, oligosaccharides were generated by *endo*- *β*-(1,4)- D-xylanase digestion of the AIR and analyzed by MALDI-TOF mass spectrometry. Based on the AIR and hemicellulose monosaccharide composition data, it was assumed that xylan/ AX/ GAX are the most abundant cell wall polymers in *Selaginella* species. As shown in Fig. 5, treatment

with the enzyme resulted in the release of fragments composed of 4 to 8 pentoses eventually branched with one 4-*O*-Me-GlcA. These data were further confirmed by Electrospray Ionisation - MS^n ($ESI\text{-}MS^n$) (data not shown). Altogether, the results indicate the presence of GAX in which the β-(1,4)-xylan is substituted with Ara and 4-*O*-Me-β-GlcA. In contrast to XyG, Xyl residues were harboring *O*-acetyl groups (from one to five) (Schultink et al., 2014) (Fig. 5A-C). Comparison of the ion relative intensity revealed that low molecular weight oligosaccharides were predominantly found in hydrated *S. involvens* (Fig. 5A). GAX fragments were not larger than 6 pentoses, whereas fragments with 7 pentoses were detected in desiccated *S. involvens*. In *S. moellendorfii* and *S. kraussiana*, oligosaccharides containing up to 8 pentoses were detected. Comparison of the relative abundance of GAX revealed a significant decrease of the fragment $Pent_5MeGlcOAc_2$ in *S. moellendorffii* and an increase in the oligo-pentose fragments $Pent_4$ and $Pent_5$ in *S. kraussiana* under dehydrated conditions. Moreover, the same structures were detected in the cell wall of both species (Fig. 5B, 5C, Fig. S3A) except that the fragments containing a terminal hexose (*i.e.*, $Pent_nMeGlcAHex$) which were found only in the hydrated *S. involvens* (Fig. 5A, Fig. S3B). Analysis of the monosaccharide composition of oligoxylan fractions confirmed that Xyl, Ara and Gal were the major sugars. Man was also detected in a non-negligible amount indicating that mannan was also present in the fraction. Moreover, the level of Gal was significantly higher in hydrated leaves from *S. involvens*, whereas Xyl content increased during desiccation (Fig. S4). Reis and co-workers (2005) have obtained xylo-oligosaccharides $Pent_nMeGlcAOAc_n$ and $Pent_nMeGlcAOAc_nHex$ by partial acid hydrolysis of *Eucalyptus globulus* wood glucuronoxylans. $Pent_nMeGlcAOAc_nHex$ oligosaccharide has been isolated only from the secondary cell wall of *Eucalyptus grandis*. In this *genus*, β-Gal*p*-(1,2)-MeGlcA and α-L-Ara*p*-(1,2)-MeGlcA side chains were found, but the role of these disaccharides in xylan function is currently unknown (Peña et al., 2016). Further studies are required to understand the functional properties of this unique structural diversity.

3.5. Structural analysis of XyG

XyG is a polysaccharide that has important roles in the structure and function of the cell wall in relation to plant development. Hydrated and desiccated crude cell wall material from leaves of three species of *Selaginella* were treated separately by *endo*-(1,4*)*-β-D-glucanase. This enzymatic hydrolysis of the AIR resulted in the release of 5 predominant XyG-derived oligosaccharides in both *S. moellendorffi* and *S. involvens*. These fragments were in decreasing numbers of their respective relative abundance: XXXG, XXFG, XLFG, XXGG/GXXG and XLXG/XXLG (Table 1). These results indicate that XyG of these two species is mostly made of a XXXG-type that can be galactosylated and fucosylated. These structures are commonly found in eudicots primary cell wall XyG (Pauly & Keegstra, 2016). Comparison of the ion relative abundance did not reveal any major difference in XyG oligosaccharides between hydrated and desiccated leaves neither in *S. moellendorffii* nor in *S. kraussiana*. However, desiccation induced an increase of XXXG and a decrease of XXFG fragments in *S. involvens* suggesting a significant change in the structure of the XXXG-type XyG during dehydration in *S. involvens* (Table 1). The significance of this modification is not yet known but we speculate that it might be related to the mechanical properties and stability of the cell wall during dehydration.

XyG is known to regulate the expansion of the cell wall by cross-linking cellulose microfibrils together. The extent of this binding is known to depend on the activity of the cell wall expansin that is able to unlock the cellulose-XyG network. Interestingly, *EXPANSIN* genes are also often transcriptionally upregulated under desiccation conditions (Jones & McQueen-Mason, 2004). Upon environmental stresses such as drying, XyG may, therefore, form an essential network, in relation with cellulose, that enables cell wall to adjust its structural organization and counteract dehydration stress (Woodenberg, Pammenter, Farrant, Driouich, & Berjak, 2014). Early studies on *C. wilmsii* have highlighted XyG remodeling (Vicré et al., 1999; Vicré et al., 2004) as important cell wall responses, while in the sister species, *C. plantagineum*, EXPANSIN have been implicated in improving extensibility during desiccation (Jones & McQueen-Mason, 2004). Altogether, these data indicate that modulation of XyG structure and its role in forming the XyG-cellulose network in the cell wall is a major cell process of desiccation tolerance in plants. In contrast and interestingly, analysis of the XyG in *S. Kraussiana* generated 9 ions that correspond mostly to Ara-containing oligosaccharides including XDDG and XXDG/XDXG (Fig. S7, Fig. S8). No Ara-containing fragments were detected in the other two species. These two XyG fragments were predominant

(representing around 70% of total XyG oligosaccharides present in the cell wall of *S. kraussiana*; Table 1). Two other Ara-containing fragments XDEG and XLEG/XELG were also present although in minor levels (Table 1). However, other structures could also be considered. In addition, XXXG and XXFG oligosaccharides were also found in *S. kraussiana* representing less than 5% of the XyG oligosaccharides from this species. Our data demonstrate that *S. kraussiana* contains an Ara-enriched XyG that is rarely found in plant cell walls. The type and order of XyG substituents are known to vary depending on the plant species, cell type and the developmental state (Pauly & Keegstra, 2016). So far, 24 structures have been identified in different plant species and described with their own one-letter designation code. In *Selaginella* species, typical structures of fucogalactoXyG were found including XXXG, XLXG/XXLG, XLFG or XLLG. *S. kraussiana* XyG contains alternative sugars unlike XyG in *S. moellendorffii* and *S. involvens*, which contain galactosyl and fucosyl substituents, instead of the galactosyl moiety at the *O*-2 position, an arabinopyranose is found on the xylosyl residue (Pena et al., 2008, Pauly & Keegstra, 2016). Consistent with this, our data show that the *S. Kraussiana* contains 9 ions most of which are arabinopyranose-containing oligosaccharides including XDXG/XXDG, XDDG, XLDG/XDLG and XDEG (Pena et al., 2008; Peña et al., 2016). Interestingly, these D-type XyG oligosaccharides represent around 75% of the total oligosaccharides released after the cell wall digestion. These data demonstrate that only *S. kraussiana* contains an Ara-enriched XyG that is rarely found in plant cell walls. Indeed, the Ara*p* residue (D) has not been found in XyG angiosperms, so far. However, the functional significance of such XyG structure in the cell walls is not known and further studies are needed to ascertain its specific role and function in the cell wall. Such data can be generated from the comparative genomic analysis of enzymes involved in XyG synthesis of *Selaginella*. However, so far only the genome of *S. moellendorffii* is sequenced. Interestingly, the *S. moellendorffii* genome contains several putative *GALACTOSYL TRANSFERASE MUR3* subclade of the GT47 (*GLYCOSYL TRANSFERASE*) and GT18 homologs which are involved in XyG side chain biosynthesis including β-D-Gal*p*A and β-D-Gal*p* transferase (Pena et al., 2008). Surprisingly, the α-L-Ara*p* transferase is also present in the genome of *S. moellendorffii* although we could not detect in our study D-containing XyG motif in this species.

3.6. Structural analysis of Mannan

Mannan is thought to be the most ancient hemicellulose among all the wall polysaccharides and has been found in the walls of several algae (Pauly et al., 2013). Mannan seems to have an

analogous structural role in the primary cell wall like XyG. As presented in Fig. 2, the relatively high level of Man in the cell wall of the three *Selaginella* species suggests the presence of mannan. This was confirmed by immunoslot-blot assay using a specific mAb LM21 (Lee et al., 2012) (Fig. S2). The structure of this polymer was investigated by treating the cell wall with an *endo*-(1,4)-β-D-mannanase followed by MALDI-TOF-MS analysis. First, the monosaccharide composition of the released oligosaccharides revealed the presence of Man as a major sugar but also the presence of Glc, Gal, Xyl and Ara (Fig. S9). In addition, MALDI-TOF-MS analysis revealed the presence of a large variety of mannan-oligosaccharides containing 3 to 7 hexoses that are either *O*-acetylated or not (Table S1). Comparison of the relative abundance of the oligomannans did not reveal any difference between hydrated and desiccated *S. moellendorffii*, *S. involvens* and *S. kraussiana* (Table S1). However, the major ions differed between the species. The ion at *m/z* 527 (Hex_3) and the one at *m/z* 569 (Hex_3OAc_1) were significantly predominant in *S. moellendorffii* and *S. involvens*, respectively. Both ions represented more than 40% of the total mannan ions present in each species. In *S. kraussiana*, the same ions represented 20 and 30% of the total mannan ions, respectively. The *O*-acetylation status of the mannan fragments was higher in *S. involvens* than in *S. kraussiana* and *S. moellendorffii* (Table 2). In many ferns and lycopods, the cell wall contains low amounts of pectin and is enriched in mannan. This type of cell wall is classified as a Type-III wall (Silva et al., 2011). Like XyG, large proportions of mannan are usually found in storage tissues and vacuoles, as non-starch carbohydrate reserves (Bento et al., 2013, Buckeridge, 2010). Mannan polysaccharides have been proposed to bind to cellulose microfibrils and other hemicelluloses *via* hydrogen bonds (Yu et al., 2014). They can, for instance, assemble with xylan and bind cellulose in diverse ways depending on the degree and nature of substituents (Whitney, Brigham, Darke, Reid, & Gidley, 1998, Kabel et al., 2007), thus influencing cell wall architecture and physical properties. Mannan seems to be an important polysaccharide in fern cell wall (Silva et al., 2011). This polysaccharide appears to serve at least two main functions: (1) the first is structural, as XyG and xylan that cross-links cellulose microfibrils, providing strength to the cell wall; and (2) the second is storage, as a non-starch carbohydrate reserve in endosperm walls and vacuoles of seeds (del Carmen Rodríguez-Gacio, Iglesias-Fernández, Carbonero, & Matilla, 2012). Moore and co-workers (2009) suggested that, like arabinogalactan proteins, mannan and galactomannan could serve as cell wall desiccation-protectants. In addition, comparison of the relative abundance of the ions revealed that the mannosyl units of galactoglucomannan are partially substituted by *O*-acetyl groups in *S. moellendorffii*, *S. involvens*, and *S. kraussiana*. In these three species, the mannosyl residue can be *O*-acetylated at the *O*-2 and *O*-3 positions.

The *O*-acetylation status of the mannan oligosaccharides was higher in *S. involvens* than in *S. kraussiana* and *S. moellendorffii*. The level of *O*-acetylation could impact the non-covalent interaction of mannan with other polymers (Gille & Pauly, 2012) like cellulose or pectin, which could result in a higher extensibility of the cell walls during dehydration. In addition, the level of *O*-acetylation of polymers seems to alter drought tolerance in Arabidopsis. It has been shown that the *Arabidopsis thaliana tbl29/esk1* mutant, in which xylan is much less acetylated than in the wild type, is more tolerant to drought (Lefevre et al., 2011). However, the enzymes that catalyze mannan *O*-acetylation are unknown (del Carmen Rodríguez-Gacio et al., 2012). Additionally, a higher degree of backbone substitution has been associated with increased polymer solubility, gelation, and enzymatic accessibility of polysaccharides *in vitro* (Schultink, Naylor, Dama, & Pauly, 2015). When some of the mannose residues are replaced by Glc residues, as in the glucomannan, or substituted with Gal as in galactomannan, the water-solubility of the polymer increases substantially. Reports suggest that galactomannan is known to retain large amounts of water (Reid & Bewley, 1979). These polymers with different levels of substitution can interact with cellulose. For instance, low level of substitutions by galactose of galactomannan promotes cross-linking with cellulose microfibrils. In contrast, high level of galactosyl substitution in galactomannan prevents this type of interaction (Schultink et al., 2015).

4. Conclusion

Our findings show that 1) leaf cell walls of the three Selaginella species are mainly composed of hemicellulosic polysaccharides (i.e., arabinoxylan and mannan), 2) the level of arabinose residues increases significantly in desiccated S. involvens when compared to desiccated S. moellendorffii and S. kraussiana, 3) the branching of xylan backbone increases in S. involvens during desiccation, 4) the level of Gal is significantly higher in hydrated leaves of S. involvens, whereas the Xyl content increases during desiccation, 5) the structure of XyG in S. involvens is modified during desiccation, 6) the XyG structure in S. kraussiana is a XDDG-type that is rarely found in plants, whereas the XyG structure of S. involvens and S. moellendorffii is of a classical XXXG-type and finally 7) O-acetylation status of mannan fragments is higher in S. involvens than in other species (Table 3).

Acknowledgments

The authors thank Yasmina Ramdani of the laboratory Glyco-MEV for her technical help in scanning electron microscopy analysis and the CEFIPRA for financial support. MALDI-TOF data were obtained on PRIMACEN (http://www.primacen.fr), the Cell Imaging Platform of Normandy, IRIB, Faculty of Sciences, University of Rouen, 76821 Mont-Saint-Aignan Cedex.

Funding

This work was supported by the Indo-French Centre for the Promotion of Advanced Research-CEFIPRA (Grant number 5300-B1 to A.D.). This work was partly supported by the University of Rouen Normandie (URN), Fédération de Recherche "Normandie-Végétal"-FED 4277, the Labex SynOrg (ANR-11-LABX-0029) and the European Regional Development Fund (ERDF 31708).

References

Banks, J. A. (2009). *Selaginella* and 400 Million Years of Separation. *Annual Review of Plant Biology*, *60*(1), 223–238.

Banks, J. A., Nishiyama, T., Hasebe, M., Bowman, J. L., Gribskov, M., dePamphilis, C., … Grigoriev, I. V. (2011). The compact *Selaginella* genome identifies changes in gene content associated with the evolution of vascular plants. *Science (New York, N.Y.)*, *332*(6032), 960–963.

Bento, J. F., Mazzaro, I., de Almeida Silva, L. M., de Azevedo Moreira, R., Ferreira, M. L. C., Reicher, F., & de Oliveira Petkowicz, C. L. (2013). Diverse patterns of cell wall mannan/galactomannan occurrence in seeds of the Leguminosae. *Carbohydrate Polymers*, *92*(1), 192–199.

Buckeridge, M. S. (2010). Seed cell wall storage polysaccharides: models to understand cell wall biosynthesis and degradation. *Plant Physiology*, *154*(3), 1017–1023.

Busse-Wicher, M., Grantham, N. J., Lyczakowski, J. J., Nikolovski, N., & Dupree, P. (2016). Xylan decoration patterns and the plant secondary cell wall molecular architecture. *Biochemical Society Transactions*, *44*(1), 74–78.

Charuvi, D., Nevo, R., Shimoni, E., Naveh, L., Zia, A., Adam, Z., … Reich, Z. (2015). Photoprotection conferred by changes in photosynthetic protein levels and organization during dehydration of a homoiochlorophyllous resurrection Plant. *Plant Physiology*, *167*(4), 1554–1565.

Deeba, F., Pandey, V., Pathre, U., & Kanojiya, S. (2009). Proteome analysis of detached fronds from a resurrection plant *Selaginella bryopteris* - response to dehydration and rehydration. *Journal of Proteomics & Bioinformatics*, *02*(02), 108–116.

del Carmen Rodríguez-Gacio, M., Iglesias-Fernández, R., Carbonero, P., & Matilla, Á. J. (2012). Softening-up mannan-rich cell walls. *Journal of Experimental Botany*, *63*(11), 695–709.

Dinakar, C., & Bartels, D. (2013). Desiccation tolerance in resurrection plants: new insights from transcriptome, proteome and metabolome analysis. *Frontiers in Plant Science*, *4*, 1–14.

Farrant, J. M., Brandt, W., & Lindsey, G. G. (2007). An overview of mechanisms of desiccation tolerance in selected angiosperm resurrection plants. *Plant Stress*, *1*(1), 72–84.

Farrant, J. M., & Moore, J. P. (2011). Programming desiccation-tolerance: from plants to seeds to resurrection plants. *Current Opinion in Plant Biology*, *14*(3), 340–345.

Farrant, J., Vander Willigen, C., Loffell, D., Bartsch, S., & Whittaker, A. (2003). An investigation into the role of light during desiccation of three angiosperm resurrection plants. *Plant, Cell and Environment*, *26*, 1275–1286.

Frei, E., & Preston, R. D. (1968). Non-cellulosic structural polysaccharides in algal cell walls. iii. Mannan in siphoneous green algae. *Proceedings of the Royal Society of London. Series B, Biological Sciences*, *169*(1015), 127–145.

Fry, S. C., & Ulvskov, P. (2011). Plant polysaccharides: biosynthesis and bioengineering. *Annual Plant Reviews*, *41*, 1–42.

Fry, S C., York, W. S., Albersheim, P., Darvill, A., Hayashi, T., Joseleau, J.-P., … White, A. R. (1993). An unambiguous nomenclature for xyloglucan-derived oligosaccharides. *Physiologia Plantarum*, *89*(1), 1–3.

Gaff, D. F., & Ellis, R. P. (1974). Southern African grasses with foliage that revives after dehydration. *Bothalia*, *11*(3), 305–308.

Gaff, D. F., & Oliver, M. (2013). The evolution of desiccation tolerance in angiosperm plants: a rare yet common phenomenon. *Functional Plant Biology*, *40*(4), 315–328.

Gille, S., & Pauly, M. (2012). *O*-acetylation of plant cell wall polysaccharides. *Frontiers in Plant Science*, *3*.

Han, Y., Li, A. xiu, Li, F., Zhao, M. Rong, & Wang, W. (2012). Characterization of a wheat (*Triticum aestivum L.*) expansin gene, *TaEXPB23*, involved in the abiotic stress response and phytohormone regulation. *Plant Physiology and Biochemistry*, *54*, 49–58.

Hsieh, Y. S. Y., & Harris, P. J. (2012). Structures of xyloglucans in primary cell walls of gymnosperms, monilophytes (ferns *sensu lato*) and lycophytes. *Phytochemistry*, *79*, 87–101.

Iturriaga, G., Cushman, M. A. F., & Cushman, J. C. (2006). An EST catalogue from the resurrection plant *Selaginella lepidophylla* reveals abiotic stress-adaptive genes. *Plant Science*, *170*(6), 1173–1184.

Jones, L., & McQueen-Mason, S. (2004). A role for expansins in dehydration and rehydration of the resurrection plant *Craterostigma plantagineum*. *FEBS Letters*, *559*(1–3), 61–65.

Lefebvre, V., Fortabat, M.-N., Ducamp, A., North, H. M., Maia-Grondard, A., Trouverie, J., … Durand-Tardif, M. (2011). ESKIMO1 Disruption in *Arabidopsis* alters vascular tissue and impairs water transport. *PLOS ONE*, *6*(2), e16645.

Lerouxel, O., Choo, T. S., Séveno, M., Usadel, B., Faye, L., Lerouge, P., & Pauly, M. (2002). Rapid structural phenotyping of plant cell wall mutants by enzymatic oligosaccharide fingerprinting. *Plant Physiology*, *130*(4), 1754–1763.

Liepman, A. H., Nairn, C. J., Willats, W. G., Sørensen, I., Roberts, A. W., & Keegstra, K. (2007). Functional genomic analysis supports conservation of function among cellulose synthase-like a gene family members and suggests diverse roles of mannans in plants. *Plant Physiology*, *143*(4), 1881–1893.

Marcus, S. E., Blake, A. W., Benians, T. A. S., Lee, K. J. D., Poyser, C., Donaldson, L., … Knox, J. P. (2010). Restricted access of proteins to mannan polysaccharides in intact plant cell walls. *The Plant Journal: For Cell and Molecular Biology*, *64*(2), 191–203.

McCartney, L., Marcus, S. E., & Knox, J. P. (2005). Monoclonal antibodies to plant cell wall xylans and arabinoxylans. *Journal of Histochemistry & Cytochemistry*, *53*(4), 543–546.

Mollet, J.-C., Park, S.-Y., Nothnagel, E. A., & Lord, E. M. (2000). A lily stylar pectin is necessary for pollen tube adhesion to an *in vitro* stylar matrix. The Plant Cell *12*(9), 1737–1750.

Moore, J. P., Le, N. T., Brandt, W. F., Driouich, A., & Farrant, J. M. (2009). Towards a systems-based understanding of plant desiccation tolerance. *Trends in Plant Science*, *14*(2), 110–117.

Moore, J. P., Nguema-Ona, E., Chevalier, L., Lindsey, G. G., Brandt, W. F., Lerouge, P., … Driouich, A. (2006). Response of the leaf cell wall to desiccation in the resurrection plant *Myrothamnus flabellifolius*. *Plant Physiology*, *141*(2), 651–662.

Moore, J. P., Nguema-Ona, E. E., Vicré-Gibouin, M., Sørensen, I., Willats, W. G., Driouich, A., & Farrant, J. M. (2013). Arabinose-rich polymers as an evolutionary strategy to plasticize resurrection plant cell walls against desiccation. *Planta*, *237*(3), 739–754.

Moore, J. P., Nguema-Ona, E. E., Vicré-Gibouin, M., Sørensen, I., Willats, W. G. T., Driouich, A., & Farrant, J. M. (2012). Arabinose-rich polymers as an evolutionary strategy to plasticize resurrection plant cell walls against desiccation. *Planta*, *237*(3), 739–754.

Moore, J. P., Vicré-Gibouin, M., Farrant, J. M., & Driouich, A. (2008). Adaptations of higher plant cell walls to water loss: drought vs desiccation. *Physiologia Plantarum*, *134*(2), 237–245.

Mouille, G., Witucka-Wall, H., Bruyant, M.-P., Loudet, O., Pelletier, S., Rihouey, C., … Pauly, M. (2006). Quantitative trait loci analysis of primary cell wall composition in Arabidopsis. *Plant Physiology*, *141*(3), 1035–1044.

Oliver, M. J., Tuba, Z., & Mishler, B. D. (2000). The evolution of vegetative desiccation tolerance in land plants. *Plant Ecology*, *151*(1), 85–100.

Pampurova, S., & Van Dijck, P. (2014). The desiccation tolerant secrets of *Selaginella lepidophylla*: What we have learned so far? *Plant Physiology and Biochemistry*, *80*, 285–290.

Pandey, V., Ranjan, S., Deeba, F., Pandey, A. K., Singh, R., Shirke, P. A., & Pathre, U. V. (2010). Desiccation-induced physiological and biochemical changes in resurrection plant, *Selaginella bryopteris*. *Journal of Plant Physiology*, *167*(16), 1351–1359.

Pauly, M., Gille, S., Liu, L., Mansoori, N., de Souza, A., Schultink, A., & Xiong, G. (2013). Hemicellulose biosynthesis. *Planta*, *238*(4), 627–642.

Pauly, M., & Keegstra, K. (2016). Biosynthesis of the plant cell wall matrix polysaccharide xyloglucan. *Annual Review of Plant Biology*, *67*, 235–259.

Pauly, M., & Ramírez, V. (2018). New insights into wall polysaccharide *O*-acetylation. *Frontiers in Plant Science*, *9*.

Peña, M. J., Darvill, A. G., Eberhard, S., York, W. S., & O'Neill, M. A. (2008). Moss and liverwort xyloglucans contain galacturonic acid and are structurally distinct from the xyloglucans synthesized by hornworts and vascular plants. *Glycobiology*, *18*(11), 891–904.

Peña, M. J., Kulkarni, A. R., Backe, J., Boyd, M., O'Neill, M. A., & York, W. S. (2016). Structural diversity of xylans in the cell walls of monocots. *Planta*, *244*(3), 589–606.

Pedersen, H. L., Fangel, J. U., McCleary, B., Ruzanski, C., Rydahl, M. G., Ralet, M.-C., … Willats, W. G. T. (2012). Versatile high resolution oligosaccharide microarrays for plant glycobiology and cell wall research. *Journal of Biological Chemistry*, *287*(47), 39429–39438.

Plancot, B., Vanier, G., Maire, F., Bardor, M., Lerouge, P., Farrant, J. M., Loutelier-Bourhis, C. (2014). Structural characterization of arabinoxylans from two African plant species *Eragrostis nindensis* and *Eragrostis tef* using various mass spectrometric methods. *Rapid Communications in Mass Spectrometry*, *28*(8), 908–916.

Puhlmann, J., Bucheli, E., Swain, M. J., Dunning, N., Albersheim, P., Darvill, A. G., & Hahn, M. G. (1994). Generation of monoclonal antibodies against plant cell-wall polysaccharides. I. Characterization of a monoclonal antibody to a terminal alpha-(1,2)-linked fucosyl-containing epitope. *Plant Physiology*, *104*(2), 699–710.

Ray, B., Loutelier-Bourhis, C., Lange, C., Condamine, E., Driouich, A., & Lerouge, P. (2004). Structural investigation of hemicellulosic polysaccharides from *Argania spinosa*: characterisation of a novel xyloglucan motif. *Carbohydrate Research*, *339*(2), 201–208.

Reid, J. S. G., & Bewley, J. D. (1979). A dual rôle for the endosperm and its galactomannan reserves in the germinative physiology of fenugreek (*Trigonella foenum-graecum* L.), an endospermic leguminous seed. *Planta*, *147*(2), 145–150.

Reis, A., Pinto, P., Evtuguin, D. V., Neto, C. P., Domingues, P., Ferrer-Correia, A. J., & Domingues, M. R. M. (2005). Electrospray tandem mass spectrometry of underivatised acetylated xylo-oligosaccharides. *Rapid Communications in Mass Spectrometry*, *19*(23), 3589–3599.

Rodriguez, M. C. S., Edsgärd, D., Hussain, S. S., Alquezar, D., Rasmussen, M., Gilbert, T., … Mundy, J. (2010). Transcriptomes of the desiccation-tolerant resurrection plant *Craterostigma plantagineum*. *The Plant Journal*, *63*(2), 212–228.

Scheller, H. V., & Ulvskov, P. (2010). Hemicelluloses. *Annual Review of Plant Biology*, *61*(1), 263–289.

Schultink, A., Liu, L., Zhu, L., & Pauly, M. (2014). Structural diversity and function of xyloglucan sidechain substituents. *Plants*, *3*(4), 526–542.

Schultink, A., Naylor, D., Dama, M., & Pauly, M. (2015). The role of the plant-specific ALTERED XYLOGLUCAN9 protein in *Arabidopsis* cell wall polysaccharide *O*-acetylation. *Plant Physiology*, *167*(4), 1271–1283.

Silva, G. B., Ionashiro, M., Carrara, T. B., Crivellari, A. C., Tiné, M. A. S., Prado, J., … Buckeridge, M. S. (2011). Cell wall polysaccharides from fern leaves: Evidence for a mannan-rich Type III cell wall in *Adiantum raddianum*. *Phytochemistry*, *72*(18), 2352–2360.

Thomson, W. W., & Platt, K. A. (1997). Conservation of cell order in desiccated mesophyll of *Selaginella lepidophylla* ([Hook and Grev.] Spring). *Annals of Botany*, *79*(4), 439–447.

Vicré, M., Farrant, J. M., & Driouich, A. (2004). Insights into the cellular mechanisms of desiccation tolerance among angiosperm resurrection plant species. *Plant, Cell & Environment*, *27*(11), 1329–1340.

Vicré, M., Sherwin, H. W., Driouich, A., Jaffer, M. A., & Farrant, J. M. (1999). Cell wall characteristics and structure of hydrated and dry leaves of the resurrection plant *Craterostigma wilmsii*, a microscopical study. *Journal of Plant Physiology*, *155*(6), 719–726.

Vicré, M., Lerouxel, O., Farrant, J., Lerouge, P., & Driouich, A. (2004). Composition and desiccation-induced alterations of the cell wall in the resurrection plant *Craterostigma wilmsii*. *Physiologia Plantarum*, *120*(2), 229–239.

Wang, X., Chen, S., Zhang, H., Shi, L., Cao, F., Guo, L., … Dai, S. (2010). Desiccation tolerance mechanism in resurrection fern-ally *Selaginella tamariscina* revealed by physiological and proteomic analysis. *Journal of Proteome Research*, *9*(12), 6561–6577.

Webb, M. A., & Arnott, H. J. (1982). Cell wall conformation in dry seeds in relation to the preservation of structural integrity during desiccation. *American Journal of Botany*, *69*(10), 1657–1668.

Whitney, S. E. C., Brigham, J. E., Darke, A. H., Reid, J. S. G., & Gidley, M. J. (1998). Structural aspects of the interaction of mannan-based polysaccharides with bacterial cellulose. *Carbohydrate Research*, *307*(3–4), 299–309.

Woodenberg, W. R., Pammenter, N. W., Farrant, J. M., Driouich, A., & Berjak, P. (2014). Embryo cell wall properties in relation to development and desiccation in the recalcitrant-seeded *Encephalartos natalensis*. *Protoplasma*, *252*(1), 245–258.

Yobi, A., Wone, B. W., Xu, W., Alexander, D. C., Guo, L., Ryals, J. A., … Cushman, J. C. (2012). Comparative metabolic profiling between desiccation-sensitive and desiccation-

tolerant species of *Selaginella* reveals insights into the resurrection trait. *The Plant Journal*, *72*, 983–999.

Yobi, A., Wone, B. W., Xu, W., Alexander, D. C., Guo, L., Ryals, J. A., … Cushman, J. C. (2013). Metabolomic profiling in *Selaginella lepidophylla* at various hydration states provides new insights into the mechanistic basis of desiccation tolerance. *Molecular Plant*, *6*(2), 369–385.

Yu, L., Shi, D., Li, J., Kong, Y., Yu, Y., Chai, G., … Zhou, G. (2014). CELLULOSE SYNTHASE-LIKE A2, a glucomannan synthase, is involved in maintaining adherent mucilage structure in *Arabidopsis* seed. *Plant Physiology*, *164*(4), 1842–1856.

			Relative abundance (%)					
Mass *m/z*	Composition	Structures	*Sm*H	*Sm*D	*Si*H	*Si*D	*Sk*H	SkD
953	Hex_4Pent_2	XXGG/GXXG[3]	11.9±5.1[a]	12.5±3.5[a]	17.4±4.2[a]	17.8±1[a]	4.4±0.7[a]	3.3±0.7[a]
1085	Hex_4Pent_3	XXXG[3]	32.8±6[a]	39.6±3.3[a]	35±2.1[a]	43.2±4.5[b]	9.5±0.9[a]	9.3±0.9[a]
1217	Hex_4Pent_4	XXDG/XDXG[4]	-	-	-	-	28.1±1.5[a]	29.5±1.6[a]
1247	Hex_5Pent_3	XLXG/XXLG[3]	9.9±1.9[a]	9.2±1.3[a]	11.6±0.6[a]	10.4±1.3[a]	-	-
1349	Hex_5Pent_4	XDDG[4]	-	-	-	-	39.7±4.7[a]	40±3.3[a]
1363	$Hex_4Pent_4Dox_1$	XXEG[4]	-	-	-	-	5.7±2.1[a]	4.9±1.7[a]
1379	Hex_5Pent_4	XLDG/XDLG[4]	-	-	-	-	5.2±1.4[a]	5.8±1.2[a]
1393	$Hex_5Pent_3Dox_1$	XXFG[3]	24.1±4.6[a]	27.1±5.4[a]	26.7±4[a]	19.1±0.8[b]	1.9±0.9[a]	2±1[a]
1409	Hex_6Pent_3	XLLG[4]	-	-	-	-	-	-
1495	$Hex_4Pent_5Dox_1$	XDEG[4]	-	-	-	-	2.6±0.8[a]	2.7±0.9[a]
1525	$Hex_5Pent_4Dox_1$	XLEG/XELG[4]	-	-	-	-	2.4±0.8[a]	2.1±0.9[a]
1555	$Hex_6Pent_3Dox_1$	XLFG[3]	15.5±3.5[a]	11.4±1.7[a]	11.8±5[a]	8.9±2.2[a]	-	-

XyG oligosaccharides were analyzed by MALDI-TOF / Mass Spectrometry. The oligosaccharides were ionized as sodium adducts.

[a,b] Data are presented as means ± SE ($n = 3$ different cell wall extracts). The values with different letters are significantly different ($p < 0.05$). Statistical analyses compared the values between desiccated and hydrated plants (Mann-Whitney test).

[1] Mass of the XyG fragments

[2] Hex, hexose; Pent, pentose; Dox, deoxyhexose

[3] XyG oligosaccharide structures described by Lerouxel *et al*. (2002).

[4] XyG oligosaccharide structures described by Peña *et al.* (2008).

Table 1. Relative abundance of XyG oligosaccharides released after *endo*-(1,4)-*β*-D-glucanase digestion of the AIR from hydrated (H) and desiccated (D) leaves of *S. moellendorffii* (*Sm*), *S. involvens* (*Si*) and *S. kraussiana* (*Sk*).

	*Sm*H	*Sm*D	*Si*H	*Si*D	*Sk*H	*Sk*D
Non acetylated fragments	48.2±3.6[a]	47.2±4.2[a]	7.3±0.2[b]	7±0.9[b]	32.2±4.2[c]	39.3±7[c]
OAc_1 fragments	26±0.8[a]	27.3±0.5[a]	53±2[b]	51±1.7[b]	28.3±3.5[a]	27.1±3.5[a]
OAc_2 fragments	22.7±1.2[a]	17.7±5.5[a]	36±2.2[b]	36±3.6[b]	34.3±1.5[b]	33.7±2.4[b]
OAc_3 fragments	4.3±2.6[a]	6.3±1.5[a]	3.7±0.6[a]	4.7±1.6[a]	4±2.6[a]	5.3±0.8[a]
OAc_4 fragments	1±0.8[a]	0.7±1.1[a]	nd	0.7±0.6[a]	0.3±0.6[a]	0.3±0.2[a]

Data are the mean ± SE (n = 3 different cell wall extracts).
[a,b,c] Data with different letters on the same line are significantly different ($p < 0.05$). Statistical analyses compared the values between the three *Sellaginella* species hydrated and desiccated on a same line (Kruskall-Wallis test).
OAc, *O*-acetyl substituent; nd, not detected

Table 2. Relative quantification (%) of *O*-acetylated mannan oligosaccharides released after *endo*-(1,4)-β-D-mannanase digestion of AIR from *Selaginella* species.
*Sm*H, hydrated *S. moellendorffii; Sm*D, desiccated *S. moellendorffii*; *Si*H, hydrated *S. involvens*; *Si*D, desiccated *S. involvens*; *Sk*H, hydrated *S. kraussiana; Sk*D, desiccated *S. kraussiana.*

	*Sm*H	*Sm*D	*Si*H	*Si*D	*Sk*H	*Sk*D
Ara content						
Ara / Xyl						
Relative proportion of Gal in xylans						
Composition change of XyG oligosaccharides						
Relative content of OAc in mannan						

Ara, arabinose; Gal, galactose; OAc, *O*-acetylated substituent; XyG, xyloglucan; Xyl, xylose.

Table 3. Summary of the major cell wall changes observed during desiccation of *Sellaginella* species.
*Sm*H: Hydrated *S. moellendorffii*, *Sm*D: Desiccated *S. moellendorffii*, *Si*H: Hydrated *S. involvens*, *Si*D: Desiccated *S. involvens*, *Sk*H: Hydrated *S. kraussiana*, *Sk*D; Desiccated *S. kraussiana*.